The current issue and full text archive of this journal is available at
www.emeraldinsight.com/0961-5539.htm

Mixed convection in a buoyancy-assisted two-sided lid-driven cavity filled with a porous medium

Elaprolu Vishnuvardhanarao
Indian Institute of Technology Guwahati, Guwahati, India, and
Manab Kumar Das
Department of Mechanical Engineering,
Indian Institute of Technology Kharagpur, Kharagpur, India

Received 7 March 2007
Revised 26 February 2008
Accepted 12 March 2008

Abstract

Purpose – The purpose of this paper is to consider a two-dimensional, steady, mixed convection flow in an enclosure filled with a fluid-saturated uniform porous medium. The left wall is moving down and the right wall is moving up and are maintained at cold and hot constant temperatures, respectively. The top and the bottom walls are fixed and are thermally insulated.

Design/methodology/approach – The governing equations are normalized and solved numerically with appropriate boundary conditions by finite-volume approach using third-order accurate scheme (deferred QUICK).

Findings – The study is conducted by varying the key parameters, i.e. Richardson number ($Ri = Gr/Re^2$), Darcy number ($Da = \kappa/H^2$) and Grashof number ($Gr = g\beta H^3 \Delta T/\nu^2$) and fixing Prandtl number at ($Pr = 0.71$). A parametric study is conducted and a set of streamline and isotherm plots are presented. The average Nusselt number reaches a value of 1 asymptotically when the Ri is gradually increased for Gr up to 10^3. The asymptotic value is 1.5 for $Gr = 10^4$. A heat transfer correlation is also presented.

Originality/value – The study of the mixed convection problem with lid-driven flows in enclosures will be useful in cooling of electronic devices, lubrication technologies, chemical processing equipment, etc.

Keywords Convection, Porous materials, Numerical analysis, Flow
Paper type Research paper

Nomenclature

A = area (m^2)
Da = Darcy number, κ/H^2
g = gravitational acceleration (m/s^2)
Gr = Grashof number, $g\beta\Delta TH^3/\nu^2$
H = enclosure length (m)
k_e = effective thermal conductivity of the porous medium (W/m-K)
k_s = thermal conductivity of the solid (W/m-K)
Nu = local Nusselt number
$\overline{Nu}$ = average Nusselt number
n = time level
Pr = Prandtl number, ν/α_e
Re = Reynolds number of the fluid, $(V_p H)/\nu$
Ri = Richardson number, Gr/Re^2
T = dimensional temperature (°C)
u^*, v^* = dimensional velocity components along (x^*, y^*) axes (m/s)

The helpful comments of the reviewers are sincerely acknowledged by the authors.

International Journal of Numerical Methods for Heat & Fluid Flow
Vol. 19 Nos. 3/4, 2009
pp. 329-351

0961-5539
DOI 10.1108/09615530910938317

u, v = dimensionless velocity components along (x, y) axes

x^*, y^* = dimensional Cartesian co-ordinates, m

x, y = dimensionless Cartesian co-ordinates

Greek symbols

α_e = effective thermal diffusivity of porous medium (m^2/s)

β = fluid thermal expansion coefficient

θ = dimensionless temperature, $(T - T_c)/(T_h - T_c)$

ν = effective kinematic viscosity (μ/ρ_0) (m^2/s)

κ = permeability of the porous medium (m^2)

Subscripts

c = cold wall

f = fluid

h = hot wall

1. Introduction

A considerable amount of research on convective heat transfer in fluid-saturated porous media has been carried out over the last several decades. This interest was due to many applications in packed sphere beds, high performance insulation for buildings, chemical catalytic reactors, grain storage and geophysical problems. Porous media are also of interest in relation to the geothermal systems (Cheng, 1978), drying of porous solids, solar collectors (Ideriah, 1980), furnaces and many others. Moreover, the mixed convection problem with lid-driven flows in enclosures are encountered in a variety of engineering applications including cooling of electronic devices, lubrication technologies, chemical processing equipment, float glass production (Pilkington, 1969), etc.

The mixed convection in a lid-driven cavity with a stable vertical temperature gradient was reported by Iwatsu *et al.* (1993). In that work, studies are made of flow and heat transfer of viscous fluid contained in a square cavity. The top wall is moving at a constant speed and the remaining walls kept stationary. The top wall is maintained at a higher temperature than the bottom wall and the side walls are adiabatic. Computations performed systematically for a wide range of Richardson number($0 \leq Ri \leq 10^6$) and Reynolds number ($0 \leq Re \leq 3,000$). The results indicated the effect of Richardson number on the flow field.

Mixed convection in square cavity with moving side walls is studied by Oztop and Dagtekin (2004). The governing parameters were Richardson number ($0.01 \leq Ri \leq 100$) and Prandtl number ($Pr = 0.7$). The effect of moving side walls on heat transfer was studied. For $Ri < 1$, the influence of moving walls on the heat transfer is same when they move in opposite direction regardless of the direction of moving walls. For the case of opposing buoyancy and shear forces and for $Ri > 1$, the heat transfer is some what better due to the formation of secondary cells on the walls. The flow in a cavity driven by two facing walls tangentially in opposite directions was studied by Kuhlmann *et al.* (1997). They have presented an experimental and numerical results on the steady flow in rectangular cavities. They concluded that the basic two-dimensional flow was not always unique. For low Reynolds numbers, it consists of two separate co-rotating vortices adjacent to the moving walls. The flow in a rectangular cavity driven by two facing sidewalls which move steadily in anti-parallel directions was studied by Blohm and Kuhlmann (2002). They have investigated experimentally for Reynolds number up to 1,200. They concluded that beyond a first threshold robust, steady, three-dimensional cells bifurcate supercritically out of the basic flow state. The

oscillatory instability is found to be critical if both sidewalls move with the same velocity (symmetrical driving).

Flow through a confined porous medium has been studied extensively in the last few years due to the large number of technological and industrial applications, for example in geothermal energy systems, prevention of sub-oil water pollution, storage of nuclear waste, etc. (see for instance, Kakac *et al.* (1985) and Bejan (1984)). Cheng (1978) provides an extensive review of the literature on free convection in fluid-saturated porous media with regard to applications in geothermal systems. Lid-driven cavities filled with saturated porous medium finds wide application in engineering such as heat exchangers, solar power collectors, packed-bed catalytic reactors, nuclear energy systems, etc. (Nield and Bejan, 1999; Vafai, 1984).

Early works on flow in porous media have used the Darcy law which is applicable to slow flows. When the flow velocity is relatively high and in the presence of boundary, the inertial and boundary effects become important. Vafai and Tien (1981) studied inertia and boundary effects on flow and heat transfer in porous media. The presented results give a detailed discussion on these non-Darcian effects. Lauriat and Prasad (1989) have studied the relative importance of inertia and viscous forces on natural convection in porous media via the Darcy–Brinkman–Forchheimer solutions for a differentially heated vertical cavity. Their results indicate that there exists an asymptotic convection regime where the solution is independent of the permeability of the porous matrix, or the Darcy and Forchheimer numbers.

Khanafer and Chamkha (1999) have investigated on mixed convection flow in a lid-driven cavity enclosure filled with a fluid-saturated porous medium. In their work, the Brinkman-extended Darcy equation of motion was used and influence of Richardson number and Darcy number on the flow was studied. Many authors have reported mixed convection flows with Darcian and non-Darcian effects along vertical plates embedded in porous media (e.g. Lai and Kulacki, 1991; Hsieh *et al.*, 1993; Chamkha and Al-Humoud, 2007), in confined geometries filled with porous media (e.g. Nithiarasu *et al.*, 1997, 1998; Mahmud and Fraser, 2006; Massarotti *et al.*, 2003; Saeid and Mohamad, 2005) or through ducts (Nebbali and Bouhadef, 2006). Oztop (2006) has numerically studied the combined convection heat transfer and fluid flow in a partially heated porous lid-driven enclosure. The top wall of enclosure moves from left to right with constant velocity and temperature. Heater with finite length is located on the fixed wall where its center of location changes along the walls. Parameters effective on flow and thermal fields are Richardson number, Darcy number, center of heater and heater length. The results show that the best heat transfer is formed when the heater is located on the left vertical wall. Šarler *et al.* (2004) have solved a steady-state natural convection problem in porous media by the radial basis function collocation method.

In the present study, the mixed convection flow in a square cavity filled with porous media is considered. The left wall is moving down and is maintained at a constant cold temperature whereas the right wall is moving up and is maintained at a constant hot temperature. The objective of the present work is to consider the Brinkman-extended Darcy equation of motion with the convective terms included as was used in Khanafer and Chamkha (1999). Two-dimensional numerical model is used and deferred QUICK scheme is used for convective terms to get high accuracy solutions. The governing parameters are Richardson number (Ri) and Darcy number (Da) for a range of Grashof number (Gr).

2. Problem description

The physical model which was considered is shown schematically in Figure 1. A two-dimensional square cavity of height H is filled with a fluid-saturated uniform porous medium and permeability. The left wall is moving down and the right wall is moving up. The velocities of the moving walls are equal and the directions are as shown. The top and bottom surfaces of the cavity are thermally insulated. The left and right walls are maintained at temperatures T_c and T_h, respectively, as shown in the figure. The direction of the gravitational force and $(x-y)$ co-ordinate system are also shown in the figure.

3. Governing equations

Flow is assumed to be two-dimensional, steady, laminar and the fluid is incompressible. The thermophysical properties are assumed to be constant except the body force term in the momentum equation, according to Boussinesq approximation. Radiation heat transfer is considered negligible with respect to other modes of heat transfer. Inertia effects of the porous medium is negligible which is appropriate when Reynolds number is small (Khanafer and Chamkha, 1999). Internal heat generation is negligible. By considering the assumptions mentioned above, the dimensional form of the governing equations can be written as,

$$\frac{\partial u^*}{\partial x^*} + \frac{\partial v^*}{\partial y^*} = 0 \tag{1}$$

$$u^* \frac{\partial u^*}{\partial x^*} + v^* \frac{\partial u^*}{\partial y^*} = -\frac{1}{\rho_0}\frac{\partial p^*}{\partial x^*} + \nu\left(\frac{\partial^2 u^*}{\partial x^{*2}} + \frac{\partial^2 u^*}{\partial y^{*2}}\right) - \frac{\mu u^*}{\rho_0 \kappa} \tag{2}$$

$$u^* \frac{\partial v^*}{\partial x^*} + v^* \frac{\partial v^*}{\partial y^*} = -\frac{1}{\rho_0}\frac{\partial p^*}{\partial y^*} + \nu\left(\frac{\partial^2 v^*}{\partial x^{*2}} + \frac{\partial^2 v^*}{\partial y^{*2}}\right) + g\beta(T - T_c) - \frac{\mu v^*}{\rho_0 \kappa} \tag{3}$$

$$u^* \frac{\partial T}{\partial x^*} + v^* \frac{\partial T}{\partial y^*} = \frac{k_e}{\rho_0 c_p}\left(\frac{\partial^2 T}{\partial x^{*2}} + \frac{\partial^2 T}{\partial y^{*2}}\right) \tag{4}$$

where u^*, v^* are the pore velocities in x^* and y^* directions, respectively, p^* is the fluid pressure, β is volumetric thermal expansion coefficient, κ is the permeability of the porous medium, ν, μ are effective kinematic and dynamic viscosities of the fluid, k_e and

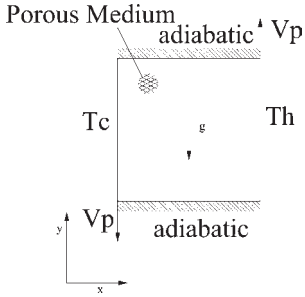

Figure 1.
Schematic diagram and boundary conditions

c_p are effective thermal conductivity and specific heat, respectively. The Equations (1)-(4) are non-dimensionalized using the following dimensionless variables.

$$x = \frac{x^*}{H}, \quad y = \frac{y^*}{H}, \quad u = \frac{u^*}{V_p}, \quad v = \frac{v^*}{V_p}, \quad p = \frac{p^*}{\rho_0 V_p^2}, \quad \theta = \frac{T - T_c}{T_h - T_c} \tag{5}$$

The resulting dimensionless equations are:

$$\frac{\partial u}{\partial x} + \frac{\partial v}{\partial y} = 0 \tag{6}$$

$$u\frac{\partial u}{\partial x} + v\frac{\partial u}{\partial y} = -\frac{\partial p}{\partial x} + \frac{1}{Re}\left(\frac{\partial^2 u}{\partial x^2} + \frac{\partial^2 u}{\partial y^2}\right) - \frac{u}{Da.Re} \tag{7}$$

$$u\frac{\partial v}{\partial x} + v\frac{\partial v}{\partial y} = -\frac{\partial p}{\partial y} + \frac{1}{Re}\left(\frac{\partial^2 v}{\partial x^2} + \frac{\partial^2 v}{\partial y^2}\right) + \frac{Gr}{Re^2}\theta - \frac{v}{Da.Re} \tag{8}$$

$$u\frac{\partial \theta}{\partial x} + v\frac{\partial \theta}{\partial y} = \frac{1}{Re.Pr}\left(\frac{\partial^2 \theta}{\partial x^2} + \frac{\partial^2 \theta}{\partial y^2}\right) \tag{9}$$

where

$$Re = \frac{V_p H}{\nu}, \quad Gr = \frac{g\beta H^3 \Delta T}{\nu^2}, \quad Da = \frac{\kappa}{H^2}, \quad Pr = \frac{\nu}{\alpha_e} \tag{10}$$

The dimensionless boundary conditions are given as:

$$\begin{array}{cc} \text{Left wall} & u = 0.0,\ v = -1.0,\ \theta = 0.0 \\ \text{Right wall} & u = 0.0,\ v = +1.0,\ \theta = 1.0 \\ \text{Top wall} & u = 0.0,\ v = 0.0,\ \dfrac{\partial \theta}{\partial y} = 0.0 \\ \text{Bottom wall} & u = 0.0,\ v = 0.0,\ \dfrac{\partial \theta}{\partial y} = 0.0 \end{array}$$

The average Nusselt number ($\overline{Nu}$) is calculated by integrating the local Nusselt number (Nu) along the left wall and is given by

$$\overline{Nu} = \int_0^1 Nu dy \tag{11}$$

where, the local Nusslet number is defined as

$$Nu = -\frac{1}{A}\frac{(\partial\theta/\partial x)_w}{\theta_h - \theta_c} \tag{12}$$

4. Numerical procedure

The governing equations (6)-(9) are discretized on a structured colocated grid. The velocity components (u,v) and the scalar variables (pressure, temperature) are located on the center of the control volume in a non-staggered manner. The governing equations are solved numerically by finite-volume method. The semi implicit method for pressure linked equation (SIMPLE) (Patankar, 1980) is used to couple the momentum and continuity equations. In the non-staggered grid, the momentum inerpolation due to Rhie and Chow (1983) has been used to avoid the checkerboard solution.

The deferred QUICK scheme of Hayase *et al.* (1990) is employed to minimize the numerical diffusion for the convective terms for both the momentum equations and energy equation. The central difference scheme of Patankar (1980) is employed near the boundary points for the convective terms. The solution of the discretized momentum and pressure correction equation is obtained by line-by-line method. The pseudo-transient approach is followed for the numerical solution as it is useful for situation in which the governing equations give rise to stability problems, e.g. buoyant flows (Versteeg and Malalasekera, 1996). The iterative procedure is initiated by the solution of energy equation followed by momentum equations and is continued until convergence is achieved. To get a converged solution, Euclidean norm was used to calculate the error (Van Doormaal and Raithby, 1984) and its value was set to 10^{-6} for dependent variable $\phi(U, V, \theta)$ and mass residual was set to 10^{-10}. An under-relaxation of 0.2 is used for pressure.

5. Code validation and grid independence study

To test and assess the grid independent solutions, numerical experiments were performed using successively sized grids, 61×61, 81×81, 101×101, 121×121 and 141×141 choosing extreme values of Richardson number ($Ri = 0.01$ and 100) and Darcy number ($Da = 10^{-4}$ and ∞). The u-velocity in the horizontal mid-plane, v-velocity in the vertical mid-plane and temperature in the horizontal mid-plane are shown in Figure 2(a)-(c), respectively. for all the grid sizes. It is observed that the curves overlap with each other for 121×121 and 141×141. So a grid number of 121×121 is chosen for further computations.

The present code is validated for mixed convection flow and heat transfer by comparing the results of a mixed convection laminar heat transfer in a lid-driven square cavity with differentially heated horizontal walls (Iwatsu *et al.*, 1993). The left and the right side walls were maintained at adiabatic condition. The top wall is kept hot while the bottom wall is cooled. In the present work numerical predictions, using the developed algorithm, have been obtained for Reynolds number (Re) = 100, Grashof number (Gr) = 100, Prandtl number (Pr) = 0.71 and Darcy number between 10^{-3} and ∞ with 121×121 grid points.

The validation of developed code was done for mixed convection flow in a lid-driven enclosure filled with a fluid-saturated porous medium problem by Khanafer and Chamkha (1999). The comparisons with the mid-plane u-velocity, mid-plane v-velocity and the mid-plane temperature are shown in Figure 3 (a)-(c) of Vishnuvardhanarao and Das (2008), respectively. The results are in very good agreement with the benchmark solution for the range of parameters considered.

6. Results and discussion

The flow and temperature distribution for mixed convection in the presence of fluid-saturated porous medium are presented here. The controlling parameters which

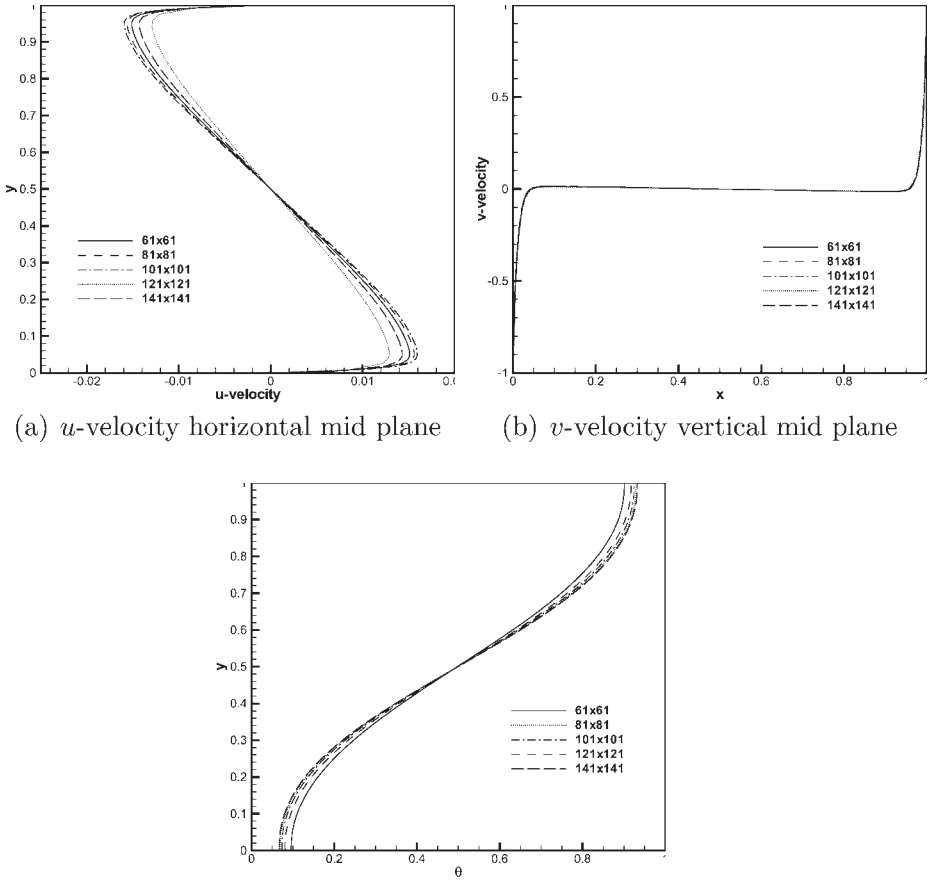

(a) u-velocity horizontal mid plane

(b) v-velocity vertical mid plane

(c) θ-velocity horizontal mid plane

Figure 2.
Grid independence study

govern the heat transfer are Richardson number, $Ri = Gr/Re^2$ (relative dominance of buoyancy to forced convection), the Darcy number, $Da = \kappa/H^2$ (the intensity of porous medium inversely). The Richardson number is varied by changing the Reynolds number while keeping the Grashof number fixed at three levels, i.e. at 10^2, 10^3 and 10^4. At each Ri, Darcy number is varied between 10^{-4} to ∞ (i.e. without the presence of porous medium). The direction of the lid-movement is shown in Figure 1. For analyzing the flow and temperature characteristics, the streamline and isotherm plots for one forced convection dominated flow ($Ri = 10^{-2}$) and the other natural convection dominated flow ($Ri = 10^2$) are presented for different Darcy numbers.

In the present case, the left lid is moving down and the right lid is moving up. The inertia force generated due to the sliding lids and the buoyancy force act in the same direction. Figures 3(a)-(e) and 4(a)-(e) represent the streamline and temperature contours respectively, for $Ri = 10^{-2}$ and $Gr = 10^2$ for different Darcy numbers. It is observed that for $Da = 10^{-4}$, most of the flow is attenuated due to the effect of porous medium and the convection is limited to near the sliding lids (Figure 3(a)) and isotherms are nearly vertical which represents conduction (Figure 4(a)). As the Darcy

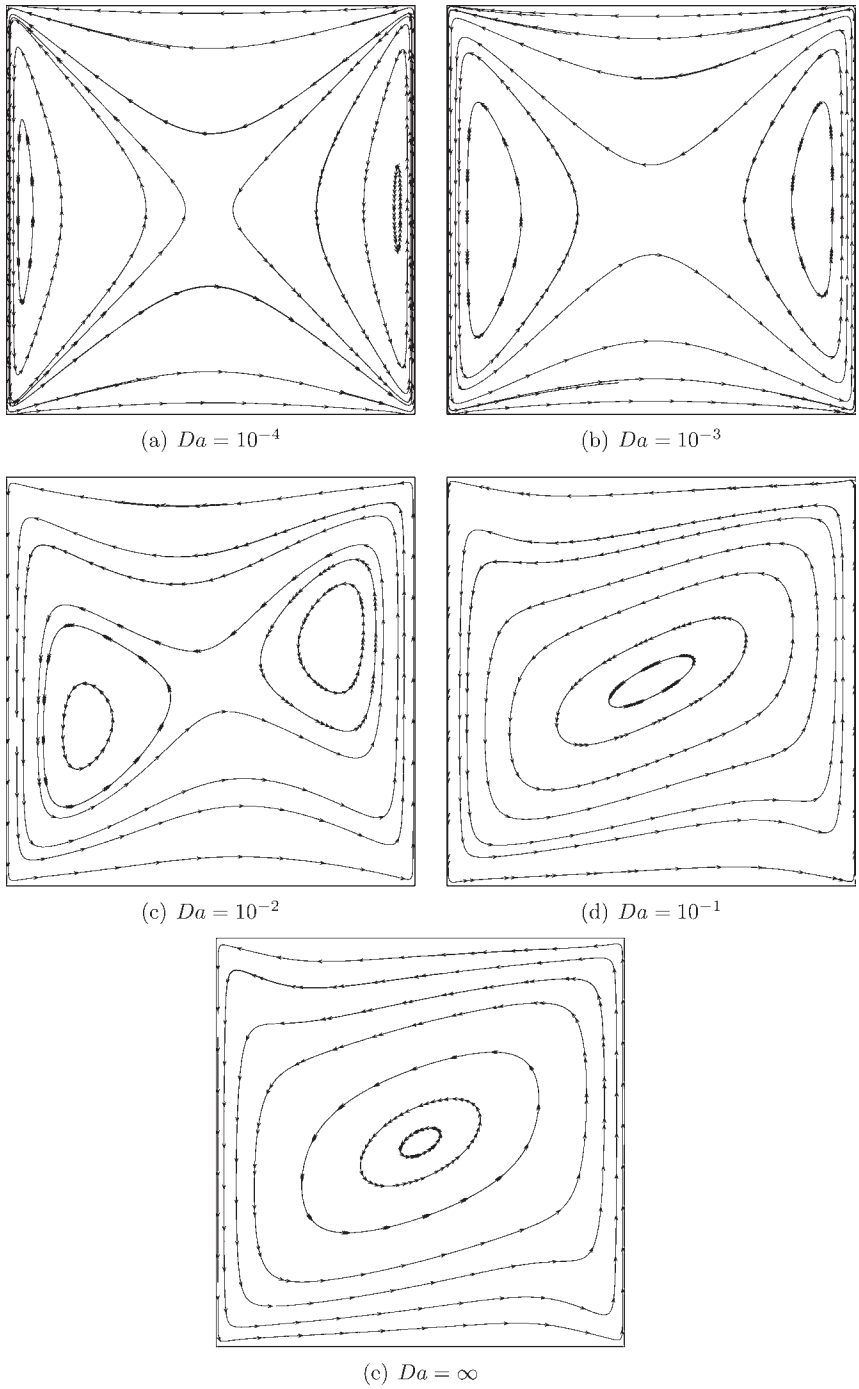

Figure 3.
Streamline plots for $Ri = 10^{-2}$, $Gr = 10^{2}$ and for various Darcy numbers (*Da*)

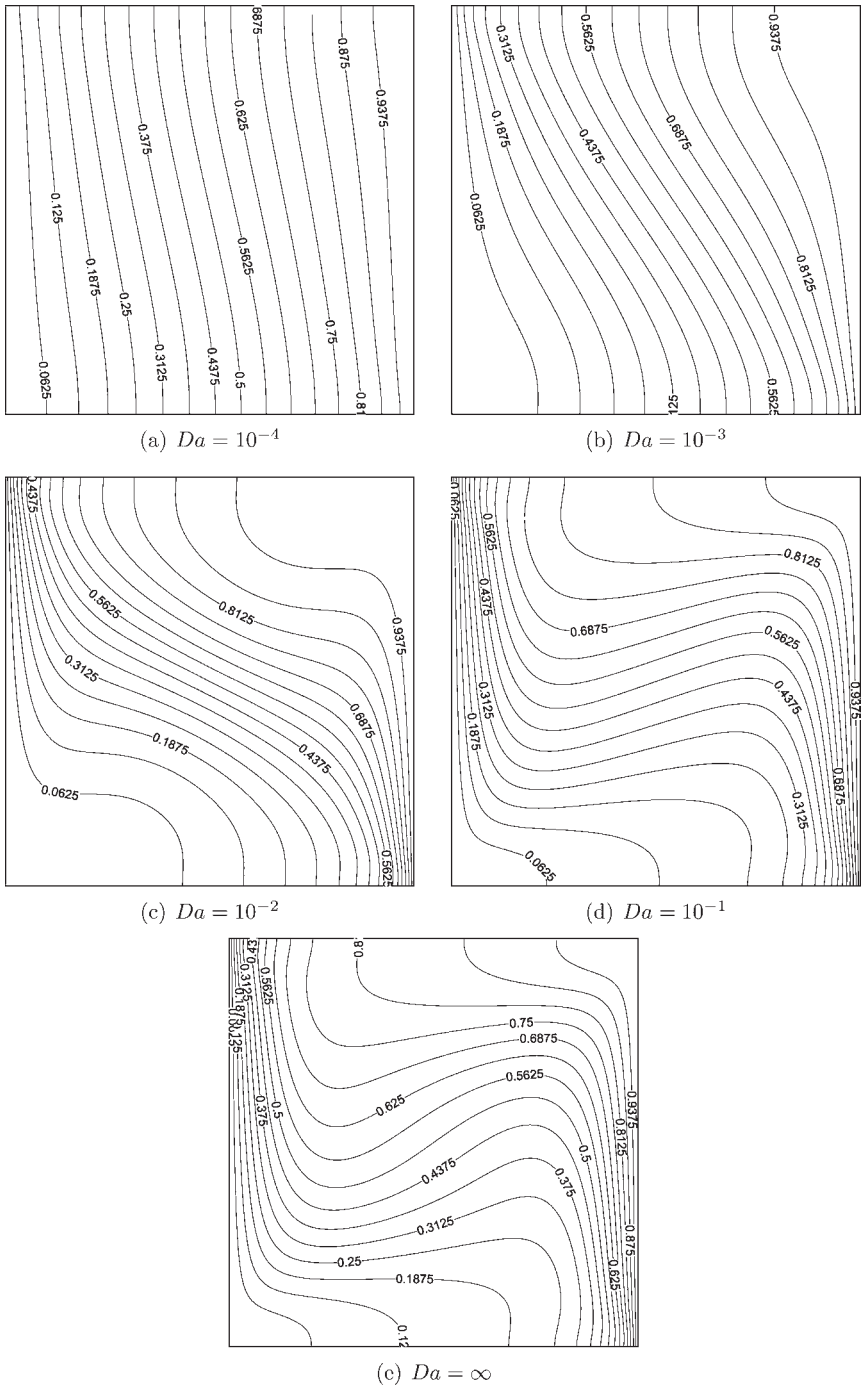

Figure 4.
Temperature contours for $Ri = 10^{-2}$, $Gr = 10^{2}$ and for various Darcy numbers (Da)

number is gradually increased, the convection domain is increased and vortices are generated near the moving-lid (Figure 3(b)). They move close to each other, finally merge and form a single vortex, which is close to the center of cavity and the direction of vortex is anti-clockwise (Figure 3(c)-(e)). The change in the shape of the isotherm is also to be noticed (Figure 4(c)-(e)). The thermal boundary layer starts forming from the top left and the right bottom signifying that the buoyancy is assisting the forced convection. As a result, the heat transfer (i.e. Nusselt number) is increased. Figures 5(a)-(e) and 6(a)-(e) represent the streamline and temperature contours respectively, for $Ri = 10^2$ and $Gr = 10^2$ for different Darcy numbers. Both the strength of natural convection ($Gr = 10^2$) and forced convection ($Re = 1$) are small. There is a single primary vortex for all Darcy numbers. The shape of the primary vortex is becoming circular one as the Darcy number increases. The two small vortices at the center merge together (Figure 5(c)). Isotherms for all Darcy numbers are nearly vertical (Figure 6(a)-(e)), which represent that the convection currents are very low. It has already been established that for $Gr < 10^3$, the heat transfer is largely by conduction only (de Vahl Davis, 1983). The corresponding heat transfer rate is also very low. Figures 7(a)-(e) and 8(a)-(e) represent the streamline and the temperature contours, respectively, for $Ri = 10^{-2}$ and $Gr = 10^4$ for different Darcy numbers. The Reynolds number is 10^3 in the present case. As the Darcy number is increased, the vortices are shifted to the corners (Figure 7(b)) and finally merge together (Figure 7(c)). The formation of two small vortices is noted, one at the top-left corner and the other at the bottom-right corner which are the culmination of the velocity boundary layers into separation. Since both the natural convection ($Gr = 10^4$) and forced convection ($Re = 10^3$) are strong and aid each other, a strong convection is noted as the Da is increased along with formation of thermal boundary layers on the side walls (Figure 8(c)-(e)). Figures 9(a)-(e) and 10(a)-(e) represent the streamline and temperature contours, respectively, for $Ri = 10^2$ and $Gr = 10^4$ for different Darcy numbers. In this case, the Reynolds number is small ($Re = 10$). The natural convection also is not strong enough which is observed by the absence of velocity boundary layer on the horizontal walls and relatively weak thermal boundary layer on the vertical walls. Figure 10(e) is similar to the one reported by de Vahl Davis (1983) where it has been concluded that the effect of natural convection is sufficient to change the mode of heat transfer from conduction to convection. Because of this, there is only a marginal increase of heat transfer in this case.

Figure 11 shows the centerline u-velocity profile along the vertical mid-plane ($x = 0.5$). High Gr corresponds to a natural convection situation and low Gr corresponds to a forced convection situation. It is observed that the u-velocity profile for $Ri = 10^2$ is larger compared to $Re = 10^{-2}$. This is because in the latter case, the flow has to overcome the adverse pressure gradient in the horizontal plane (secondary corner vortices in Figure 7(e)) and thus the reduction in velocity whereas in the former case, this is absent because of the buoyancy forces. The relative magnitude increases with increase in Gr (Figure 11(c)-(e)). With the increase in Da, velocity increases. However, after $Da = 10^{-1}$, the increment is less.

The temperature distribution in the vertical mid-plane along y is shown in Figure 12. absence of convection is represented by a vertical line. The temperature distribution for $Ri = 10^{-2}$ and $Gr = 10^2$ is shown in Figure 12(a) which increases with Gr. The pattern remains same for $Da = \infty$. However, a large isothermal core is observed for $Ri = 10^{-2}, Gr = 10^4$ because of the strong convection. The temperature for two

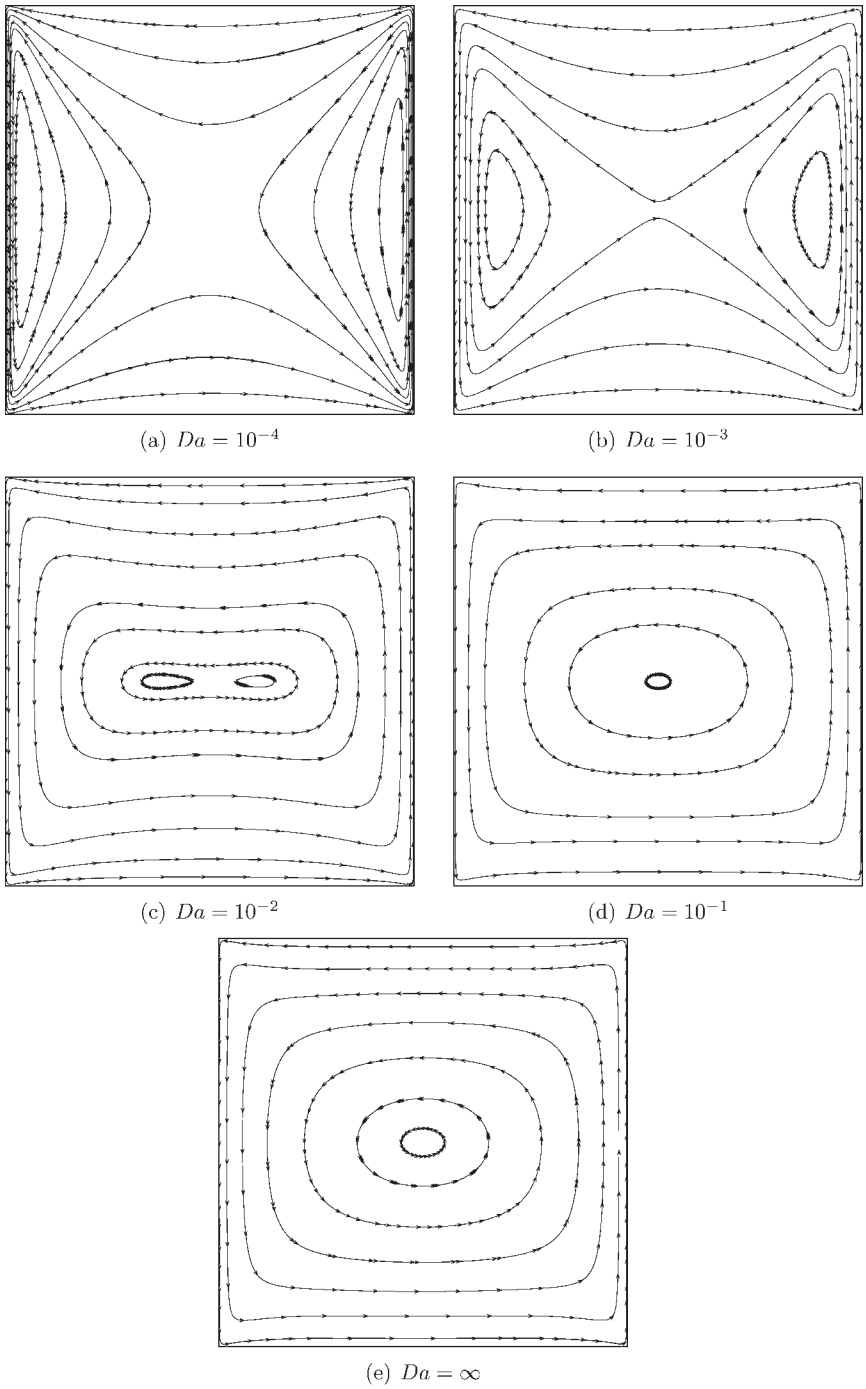

Figure 5.
Streamline plots for $Ri = 10^2$, $Gr = 10^2$ and for various Darcy numbers (Da)

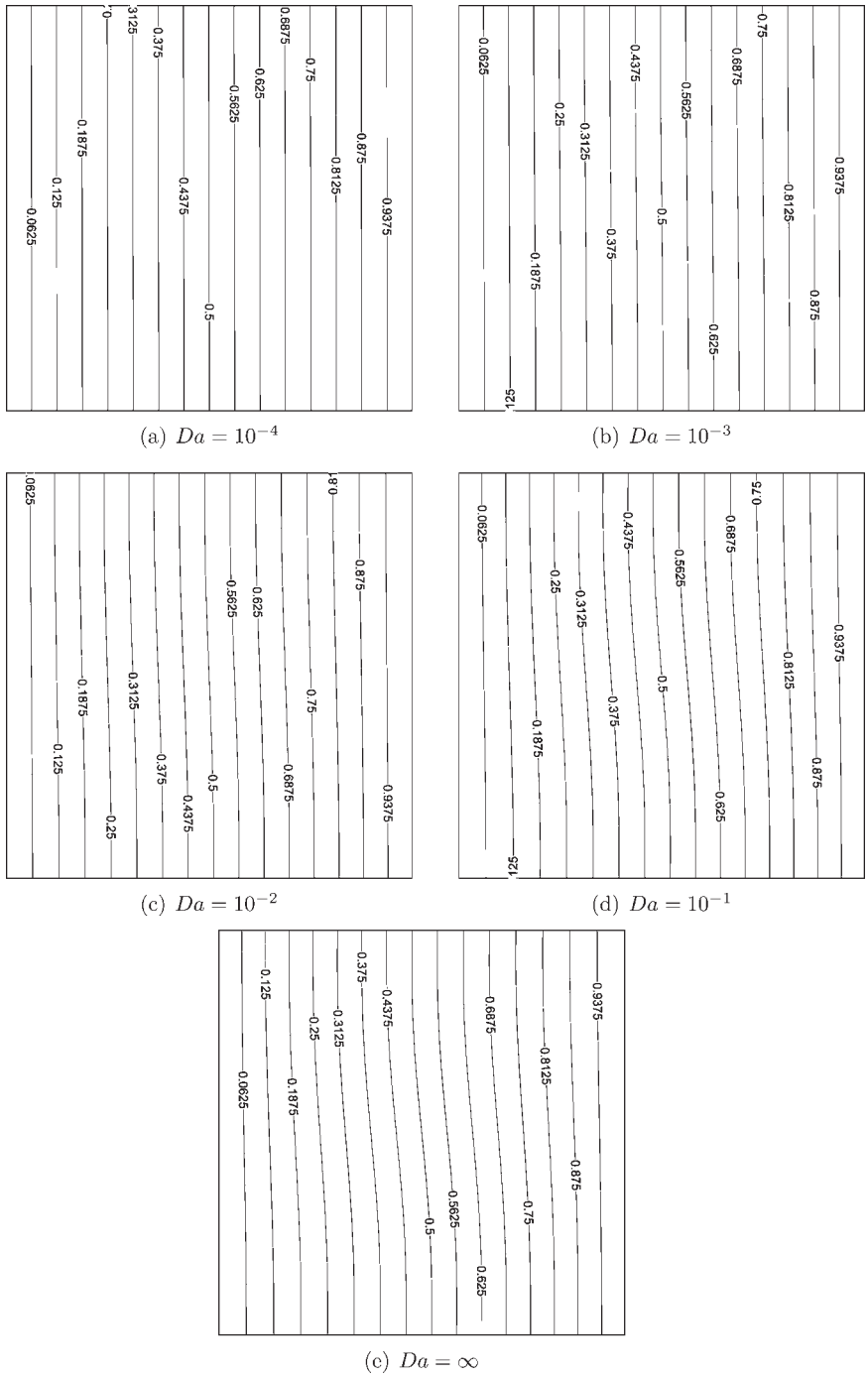

(a) $Da = 10^{-4}$

(b) $Da = 10^{-3}$

(c) $Da = 10^{-2}$

(d) $Da = 10^{-1}$

(e) $Da = \infty$

Figure 6.
Temperature contours for $Ri = 10^2$, $Gr = 10^2$ and for various Darcy numbers (Da)

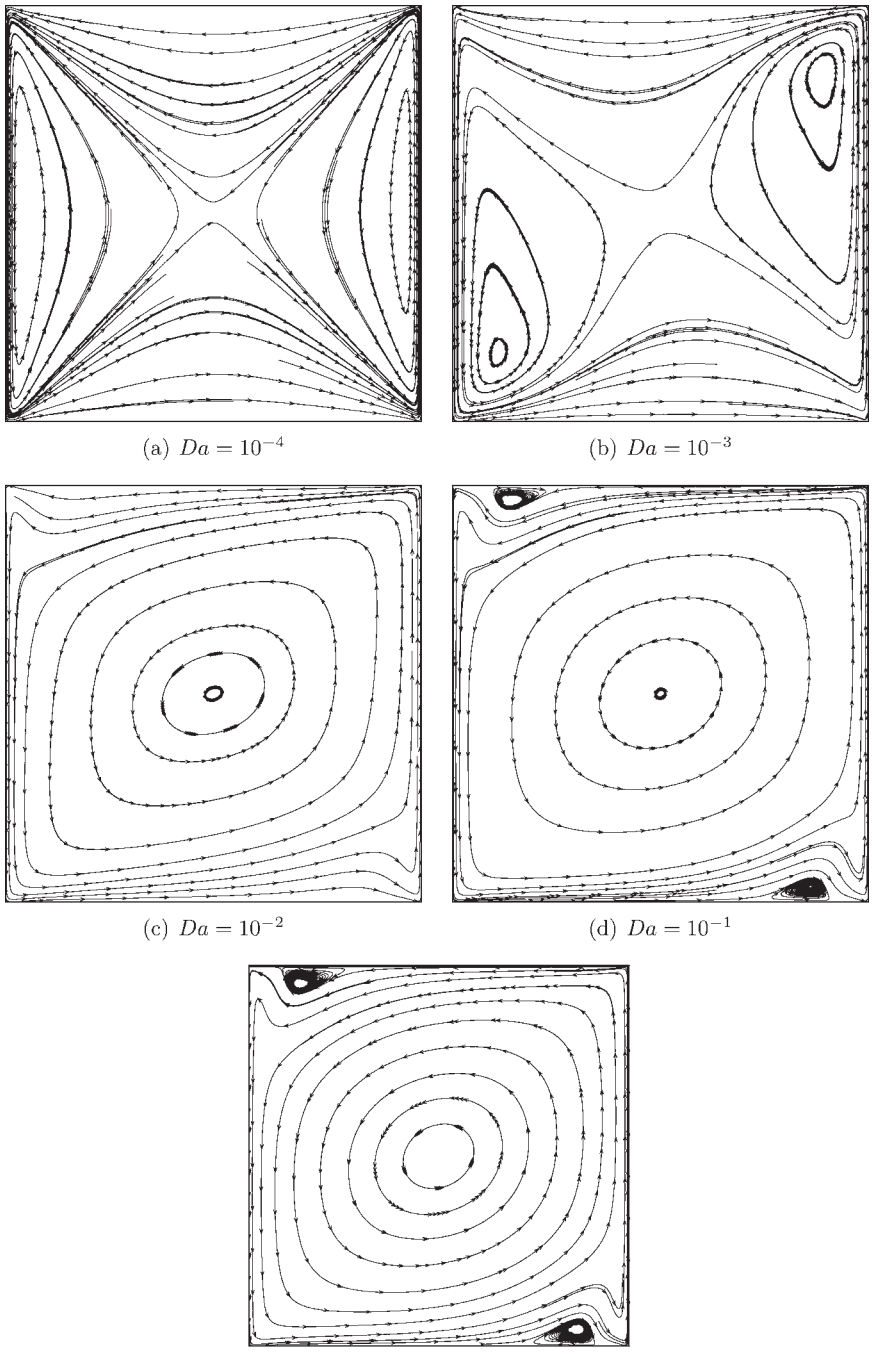

Figure 7.
Streamline plots for $Ri = 10^{-2}$, $Gr = 10^4$ and for various Darcy numbers (Da)

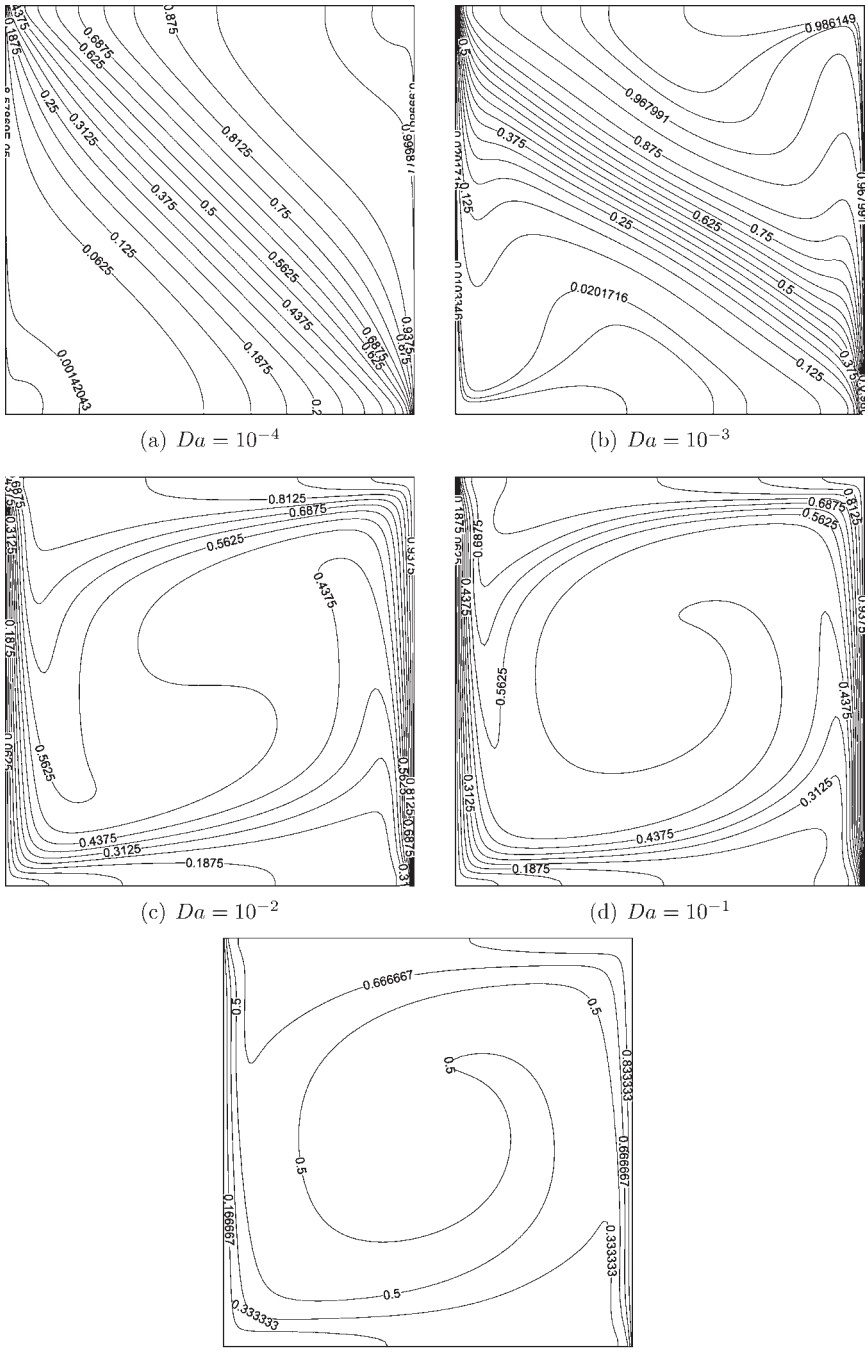

(a) $Da = 10^{-4}$ (b) $Da = 10^{-3}$

(c) $Da = 10^{-2}$ (d) $Da = 10^{-1}$

(e) $Da = \infty$

Figure 8.
Temperature contours for $Ri = 10^{-2}$, $Gr = 10^{4}$ and for various Darcy numbers (*Da*)

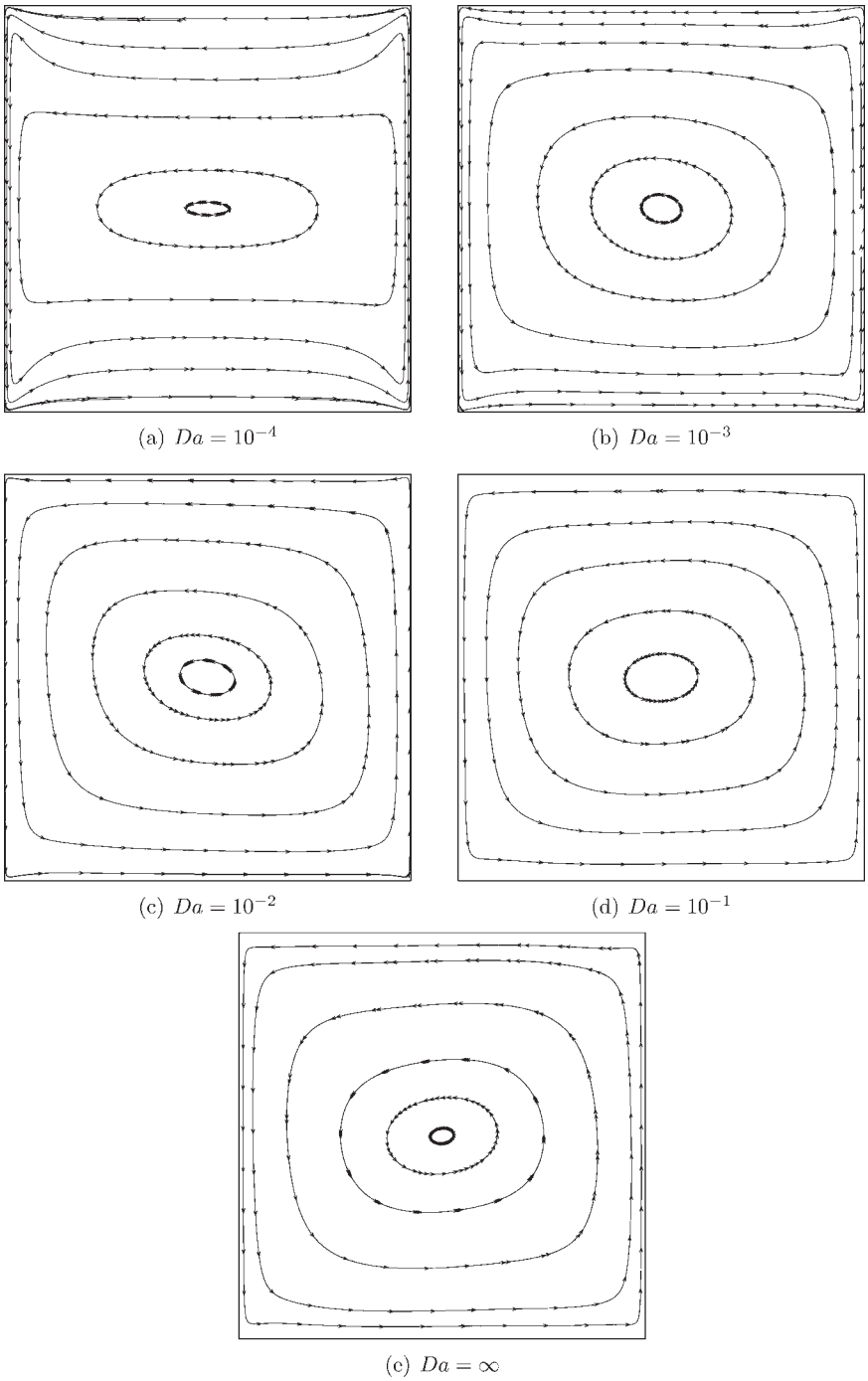

Figure 9.
Streamline plots for $Ri = 10^2$, $Gr = 10^4$ and for various Darcy numbers (Da)

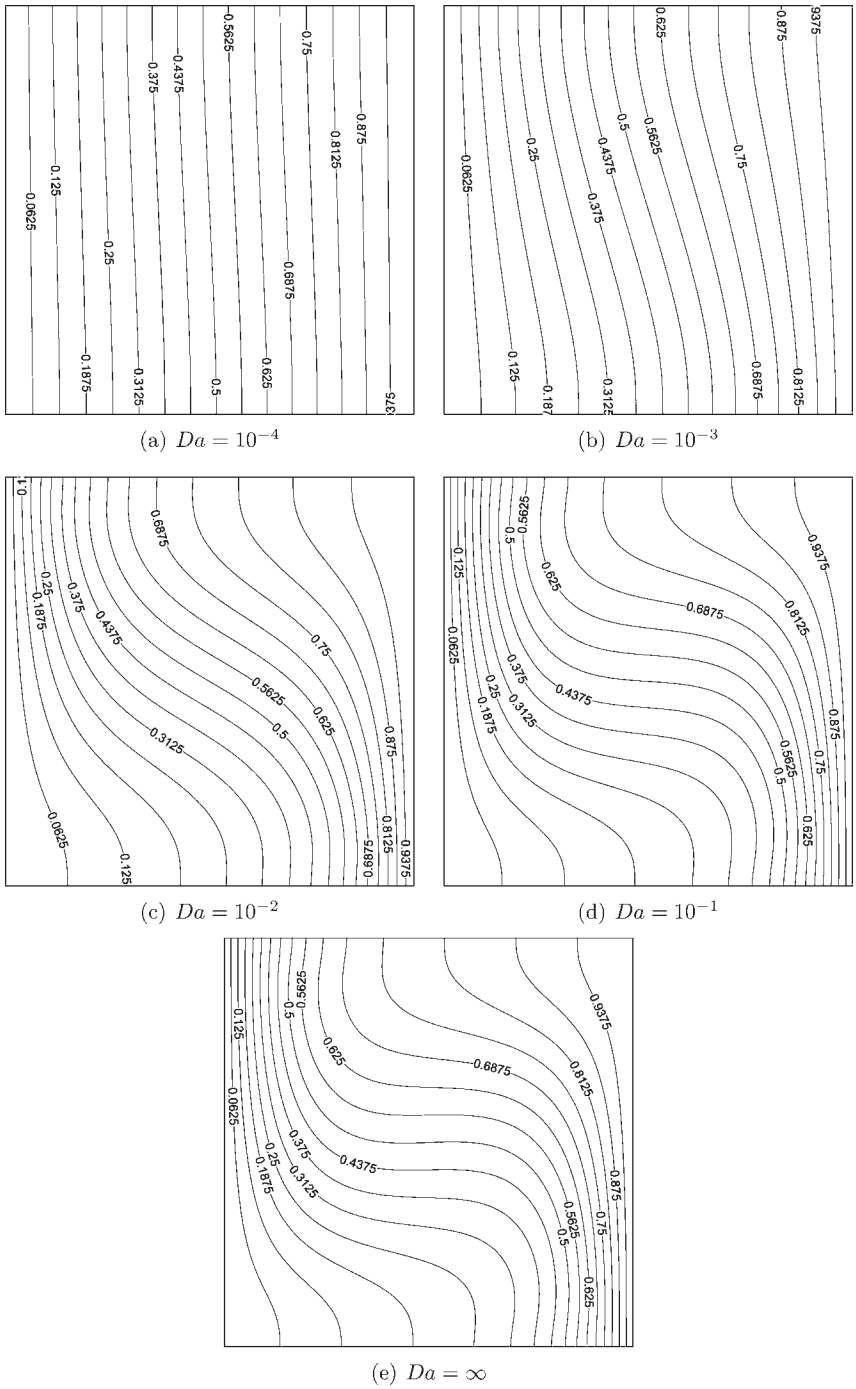

Figure 10.
Temperature contours for $Ri = 10^2$, $Gr = 10^4$ and for various Darcy numbers (Da)

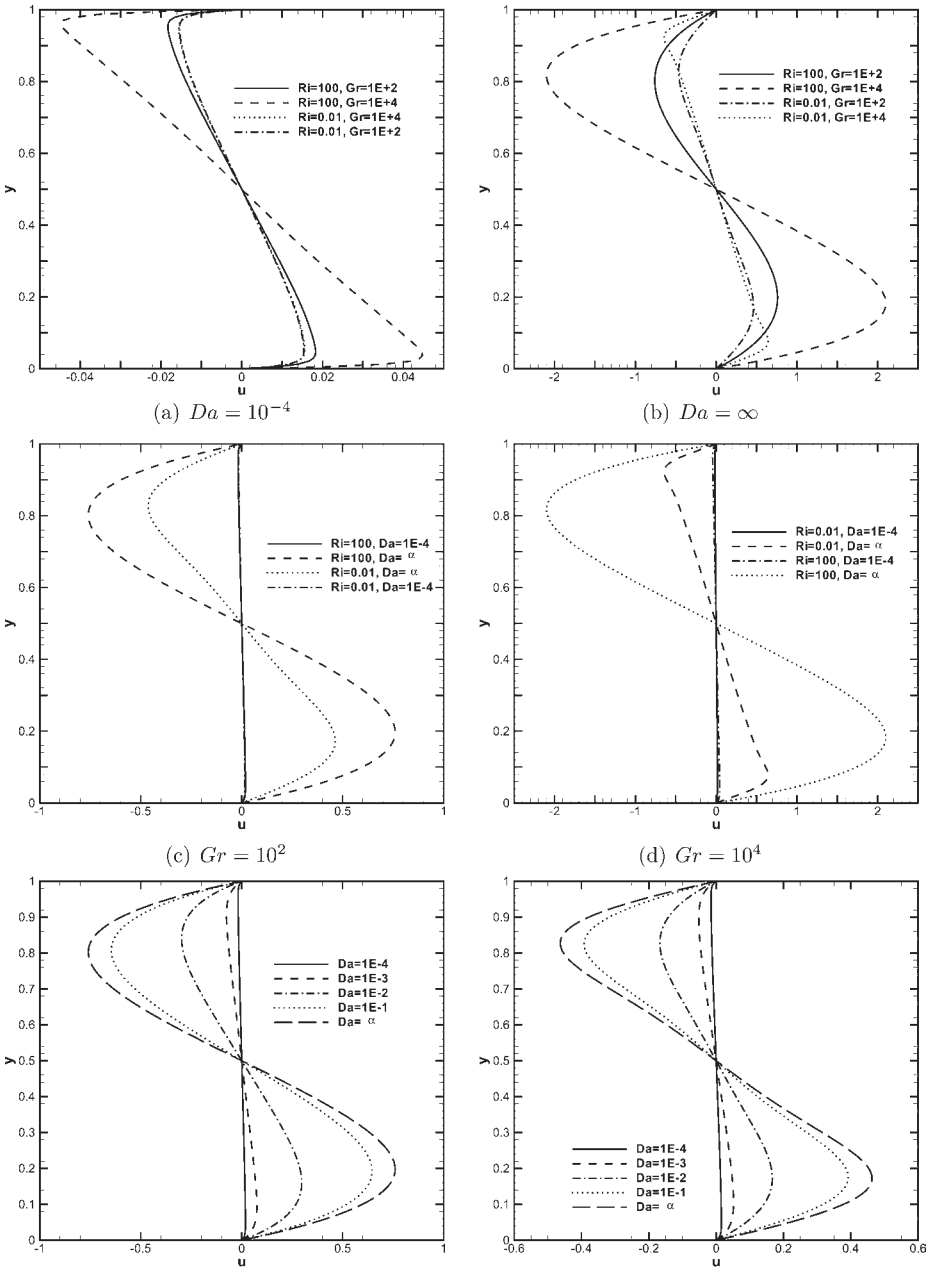

(a) $Da = 10^{-4}$ (b) $Da = \infty$

(c) $Gr = 10^2$ (d) $Gr = 10^4$

(e) $Ri = 100,\ Gr = 10^2$ (f) $Ri = 0.01,\ Gr = 10^2$

Figure 11.
u-velocity along vertical centerline

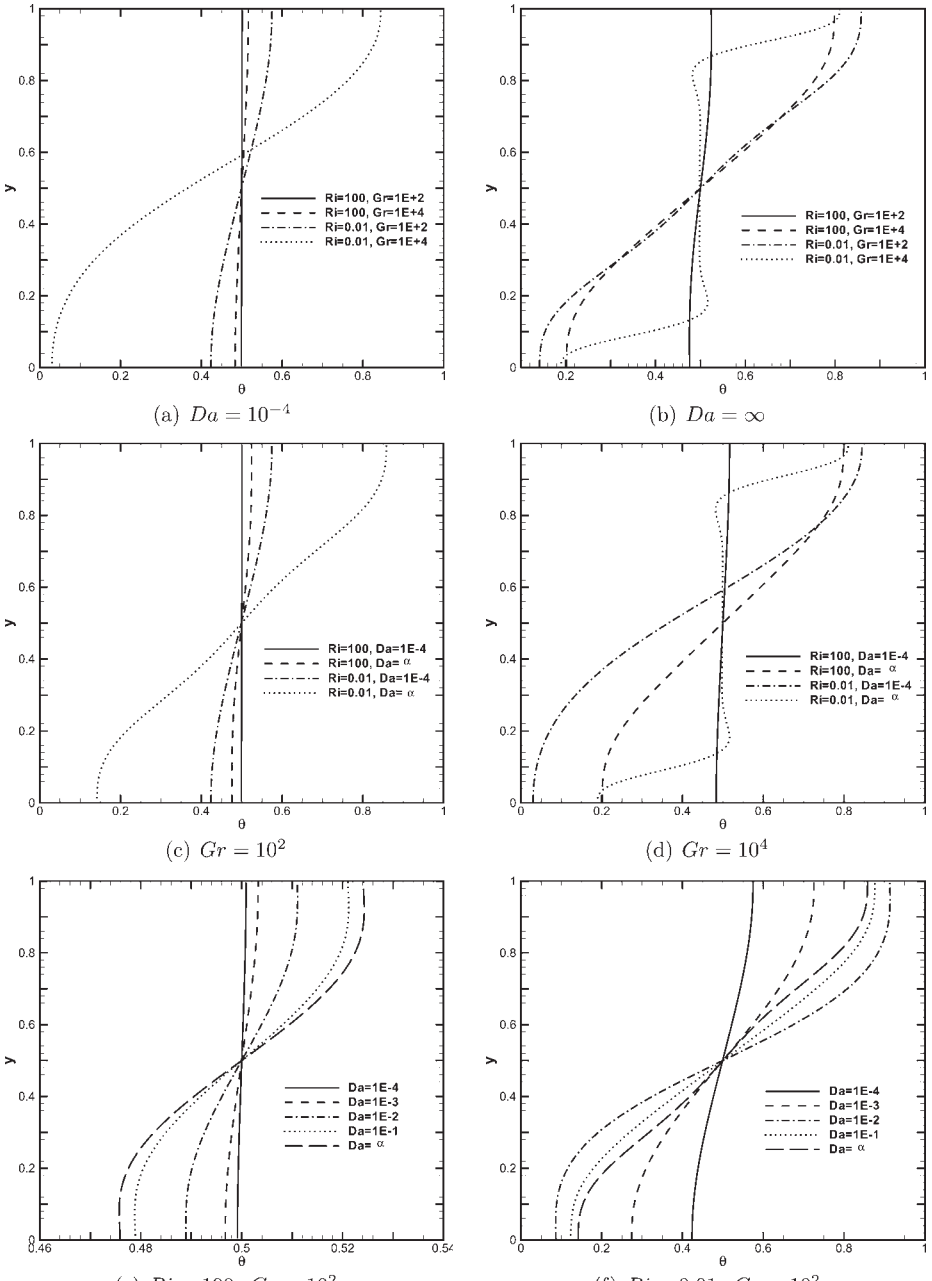

(a) $Da = 10^{-4}$

(b) $Da = \infty$

(c) $Gr = 10^2$

(d) $Gr = 10^4$

(e) $Ri = 100,\ Gr = 10^2$

(f) $Ri = 0.01,\ Gr = 10^2$

Figure 12.
Variation of temperature along vertical centerline

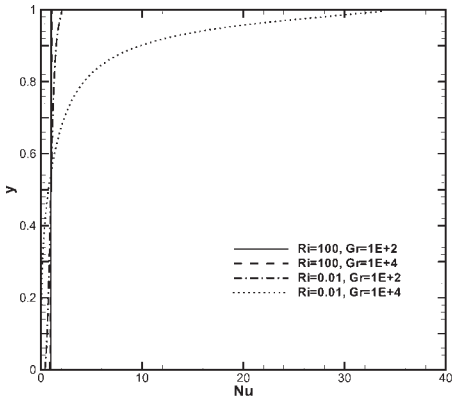

(a) $Da = 10^{-4}$

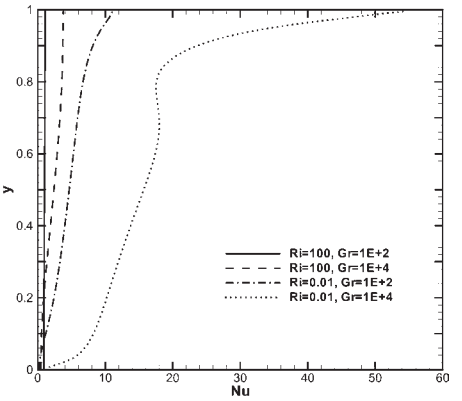

(b) $Da = \infty$

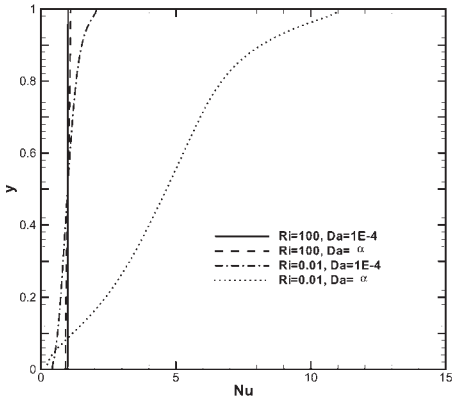

(c) $Gr = 10^2$

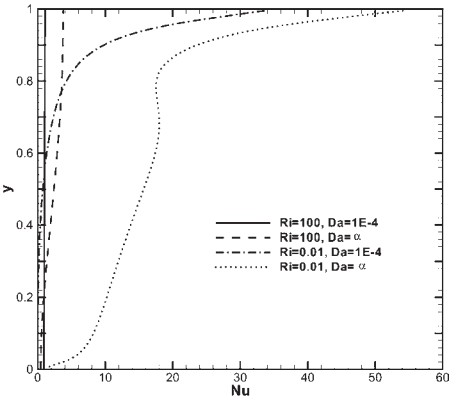

(d) $Gr = 10^4$

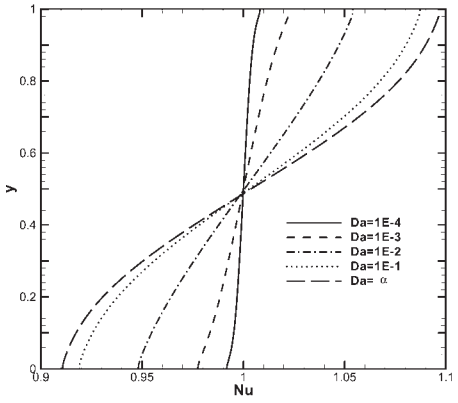

(e) $Ri = 100,\ Gr = 10^2$

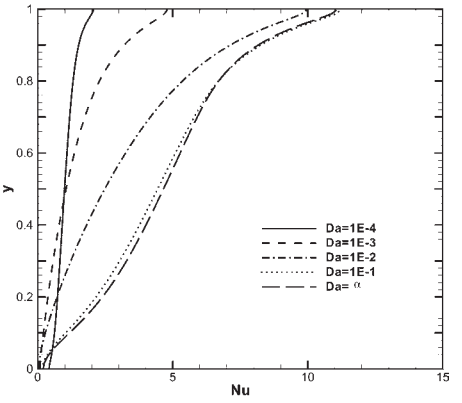

(f) $Ri = 0.01,\ Gr = 10^2$

Figure 13.
Variation local Nusselt number (Nu_y) along vertical centerline

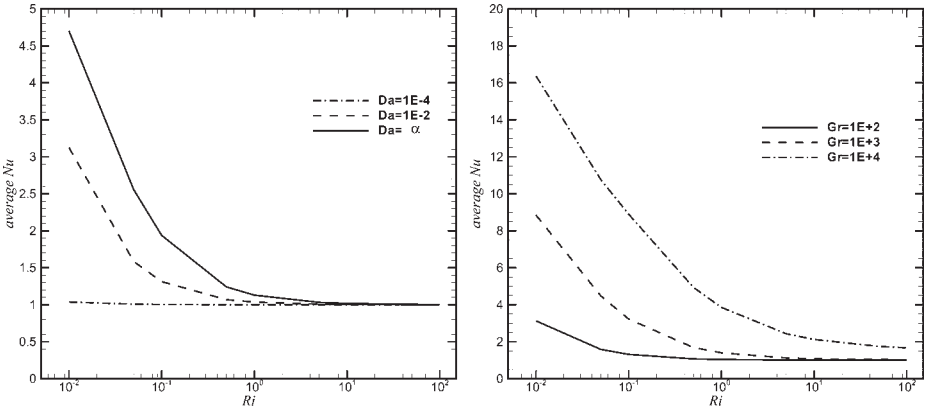

(a) $Gr = 10^2$ (b) $Da = 10^{-2}$

Figure 14.
Variation Nusselt number ($\overline{Nu}$) for different Richardson numbers (Ri)

different Gr are shown in Figure 12(c) and (d). With increase in Da, the convection increases and thus the range of temperature also increases (Figure 12(e) and (f)).

The local Nusselt number along the cold wall is shown in Figure 13. For the present case, Nu decreases from top to bottom. The Nu is high for $Da = \infty$ (Figure 13(a) and (b)). As discussed earlier, Nu is high for $Ri = 10^{-2}$ and $Gr = 10^4$. The relative increase of Nu with two Grashof numbers is shown in Figure 13(c) and (d). With the gradual increase in Da, Nu increases as shown in Figure 13(e) and (f). However, after $Da = 10^{-1}$, the change is not substantial.

Figure 14(a) shows the average Nusselt number for three Darcy numbers with $Gr = 10^2$. It is observed, that $\overline{Nu}$ increases as the Darcy number increases. For a fixed Grashof number, as the Richardson number increases, $\overline{Nu}$ for all the Darcy numbers reaches asymptotically to a same constant value and is approximately equal to one, which represents strong conduction dominated flow. But for a fixed Darcy number, as the Richardson number increases, $\overline{Nu}$ asymptotically reaches a constant value for $Gr = 10^2$ and 10^3 and is equal to 1. However, for $Gr = 10^4$, though the same trend is observed, the asymptotic value is higher and nearly equal to 1.5 (Figure 14(b)).

7. A heat transfer correlation

The numerically calculated heat transfer results were correlated for mixed convection in a square cavity and in the presence of porous medium. The average Nusselt number is correlated as a function of inverse Darcy number ($Da^{-1} = 1/Da$), the Richardson number $Ri = Gr/Re^2$ and the Grashof number. The equation is given by:

$$\overline{Nu} = 1 + \frac{0.1456}{(1 + Da^{-1})^{0.194}} (Ri)^{-0.3617} (Gr)^{0.3969} \tag{13}$$

for $10^{-4} \leq Da \leq 10^{-1}$.

8. Conclusions

Numerical study of mixed convection heat transfer in a two-dimensional enclosure filled with a fluid-saturated porous medium has been carried out. The left wall is

moving down and the right wall is moving up. The left and the right walls are under cold and hot conditions, respectively. The finite volume method using SIMPLE algorithm in a colocated grid arrangement was employed for the present problem. The deferred QUICK scheme is used to minimize the numerical diffusion. Comparisons with previously published work on special cases of the problem were performed and found to be in good agreement. The constant stream function and the temperature plots for various parametric conditions were presented and discussed. To vary the Richardson number, Grashof number is fixed at three levels, i.e. at 10^2, 10^3 and 10^4 and correspondingly Reynolds number is varied.

At low *Da*, two small vortices are formed. They merge together with increase in *Da*. In case of $Ri = 10^{-2}$, the strength of convection increases with the increase in *Gr* and formation of secondary vortices are noticed at $Gr = 10^4$. For $Ri = 10^2$, conduction is the mode of heat transfer at $Gr = 10^2$. At $Gr = 10^4$, natural convection effect is noticed. Significant suppression of the convective currents was obtained by the presence of a porous medium. The local Nusselt number distribution along the left wall increases in the positive *y*-direction. With the increase in *Ri*, the average Nusselt number approaches a value of 1 asymptotically for $Gr = 10^2$ and 10^3. This signifies that heat transfer is dominated by conduction only. This asymptotic value is 1.5 for $Gr = 10^4$. A heat transfer correlation has been proposed for average *Nu* as a function of inverse *Da*, *Ri* and *Gr*.

References

Bejan, A. (1984), *Convective Heat Transfer*, 1st ed., Chapter 11, Wiley, New York, NY.

Blohm, Ch. and Kuhlmann, H.C. (2002), "The two-sided lid-driven cavity: experiments on stationary and time-dependent flows", *Journal of Fluid Mechanics*, Vol. 450, pp. 67-95.

Chamkha, A.J. and Al-Humoud, J.M. (2007), "Mixed convection heat and mass transfer of non-newtonian fluids from a permeable surface embedded in a porous medium", *International Journal of Numerical Methods for Heat & Fluid Flow*, Vol. 17 No. 2, pp. 195-212.

Cheng, P. (1978), "Heat transfer in geothermal systems", *Advances in Heat Transfer*, Vol. 4, pp. 1-105.

de Vahl Davis, G. (1983), "Natural convection of air in a square cavity: a bench mark solution", *International Journal for Numerical Methods in Fluids*, Vol. 3, pp. 249-64.

Hayase, T., Humphrey, J.A.C. and Greif, R. (1990), "A consistently formulated QUICK scheme for fast and stable convergence using finite-volume iterative calculation procedures", *Journal of Computational Physics*, Vol. 98, pp. 108-18.

Hsieh, J.C., Chen, T.S. and Armaly, B.F. (1993), "Nonsimilarity solutions for mixed convection from vertical surface in a porous medium-variable surface temperature or heat flux", *International Journal of Heat and Mass Transfer*, Vol. 36, pp. 1485-93.

Ideriah, F.J.K. (1980), "Prediction of turbulent cavity flow driven by buoyancy and shear", *Journal of Mechanical Engineering Science*, Vol. 22, pp. 287-95.

Iwatsu, R., Hyun, J.M. and Kuwahara, K. (1993), "Mixed convection in a driven cavity with a stable vertical temperature gradient", *International Journal of Heat and Mass Transfer*, Vol. 36, pp. 1601-8.

Kakac, S., Aung, W. and Viskanta, R. (1985), *Natural Convection: Fundamentals and Applications*, Hemisphere, Washington, DC, pp. 475-611.

Khanafer, K.M. and Chamkha, A.J. (1999), "Mixed convection flow in a lid-driven enclosure filled with a fluid-saturated porous medium", *International Journal of Heat and Mass Transfer*, Vol. 42, pp. 2465-81.

Kuhlmann, H.C., Wanschura, M. and Rath, H.J. (1997), "Flow in two-sided lid-driven cavities: non-uniqueness, instabilities and cellular structures", *Journal of Fluid Mechanics*, Vol. 336, pp. 267-99.

Lai, F.C. and Kulacki, F.A. (1991), "Non-darcy mixed convection along a vertical wall in a saturated porous media", *Journal of Heat Transfer*, Vol. 113, pp. 252-5.

Lauriat, G. and Prasad, V. (1989), "Non-darcian effects on natural convection in a vertical porous enclosure", *International Journal of Heat and Mass Transfer*, Vol. 32, pp. 2135-48.

Mahmud, S. and Fraser, R.A. (2006), "Vibrational effect on heat transfer and entropy generation in an elliptic porous cavity", *International Journal of Numerical Methods for Heat & Fluid Flow*, Vol. 16 No. 2, pp. 151-71.

Massarotti, N., Nithiarasu, P. and Carotenuto, A. (2003), "Microscopic and macroscopic approach for natural convection in enclosures filled with fluid saturated porous medium", *International Journal of Numerical Methods for Heat & Fluid Flow*, Vol. 13 No. 7, pp. 862-86.

Nebbali, R. and Bouhadef, K. (2006), "Numerical study of forced convection in a 3d flow of a non-newtonian fluid through a porous duct", *International Journal of Numerical Methods for Heat & Fluid Flow*, Vol. 16 No. 8, pp. 870-89.

Nield, D.A. and Bejan, A. (1999), *Convection in Porous Media*, Springer-Verlag, New York, NY.

Nithiarasu, P., Seetharamu, K.N. and Sundararajan, T. (1997), "Natural convective heat transfer in a fluid saturated variable porosity medium", *International Journal of Heat and Mass Transfer*, Vol. 40, pp. 3955-67.

Nithiarasu, P., Seetharamu, K.N. and Sundararajan, T. (1998), "Effect of porosity on natural convective heat transfer in a fluid saturated porous medium", *International Journal of Heat and Fluid Flow*, Vol. 19, pp. 56-8.

Oztop, H.F. (2006), "Combined convection heat transfer in a porous lid-driven enclosure due to heater with finite length", *International Communications in Heat and Mass Transfer*, Vol. 33, pp. 772-9.

Oztop, H.F. and Dagtekin, I. (2004), "Mixed convection in two-sided lid-driven differentially heated square cavity", *International Journal of Heat and Mass Transfer*, Vol. 47, pp. 1761-9.

Patankar, S.V. (1980), *Numerical Heat Transfer and Fluid Flow*, Hemisphere, New York, NY.

Pilkington, L.A.B. (1969), "Review lecture: the float glass process", *Proceedings of the Royal Society*, Vol. 314, pp. 1-25.

Rhie, C.M. and Chow, W.L. (1983), "A numerical study of the turbulent flow past an isolated airfoil with trailing edge separation", *AIAA Journal*, Vol. 21, pp. 1525-32.

Saeid, N.H. and Mohamad, A.A. (2005), "Natural convection in a porous cavity with spatial sidewall temperature variation", *International Journal of Numerical Methods for Heat & Fluid Flow*, Vol. 15 No. 6, pp. 555-66.

Šarler, B., Perko, J. and Chen, C.-S. (2004), "Radial basis function collocation method solution of natural convection in porous media", *International Journal of Numerical Methods for Heat & Fluid Flow*, Vol. 14 No. 2, pp. 187-212.

Vafai, K. (1984), "Convective flow and heat transfer in variable-porosity media", *Journal of Fluid Mechanics*, Vol. 147, pp. 233-59.

Vafai, K. and Tien, C.L. (1981), "Boundary and inertia effects on flow and heat transfer in porous media", *International Journal of Heat and Mass Transfer*, Vol. 24, pp. 195-203.

Van Doormaal, J.P. and Raithby, G.D. (1984), "Enhancements of the SIMPLE method for predicting incompressible fluid flows", *Numerical Heat Transfer*, Vol. 7, pp. 147-63.

Versteeg, H.K. and Malalasekera, W. (1996), *An Introduction to Computational Fluid Dynamics. The Finite Volume Method*, Longman, New York, NY.

Vishnuvardhanarao, E. and Das, M.K. (2008), "Laminar mixed convection in a parallel two-sided lid-driven differentially heated square cavity filled with a fluid-saturated porous medium", *Numerical Heat Transfer: Part A*, Vol. 53, pp. 88-110.

Corresponding author
Manab Kumar Das can be contacted at: manab@mech.iitkgp.ernet.in